Molecular Crystals and Liquid Crystals
Publication details, including instructions for authors and subscription information:
http://www.tandfonline.com/loi/gmcl16

Surface Plasmon Enhanced Vibrational Spectra of Monolayer Assemblies on Gratings and Rough Metal Surfaces

M. R. Philpott [a], A Girlando [a b], W G. Golden [a c], W Knoll [a d] & J. D. Swalen [a]

[a] IBM Research Laboratory, 5600 Cottle Road, San Jose, CA, U.S.A.

[b] Istituto di Chimica Fisica, Universita degli Studi di Padova, 2 Via Loredan, 35100, Padova, Italy

[c] IBM Instruments Inc., 40 West Brokaw Road, San Jose, California, 95110

[d] Physik Department E22, Technische Universität München, D-8046, Garching, Fed. Rep. Germany

Version of record first published: 17 Oct 2011.

Mol. Cryst. Liq. Cryst., 1983, Vol. 96, pp. 335–351
0026-8941/83/9604–0335/$18.50/0

Printed in the United States of America

SURFACE PLASMON ENHANCED VIBRATIONAL SPECTRA OF MONOLAYER ASSEMBLIES ON GRATINGS AND ROUGH METAL SURFACES

M. R. PHILPOTT, A. GIRLANDO,* W. G. GOLDEN,**
W. KNOLL,*** J. D. SWALEN
IBM Research Laboratory, 5600 Cottle Road,
San Jose, CA, U.S.A.

Abstract The vibrational spectra of monolayer assemblies of cadmium arachidate on smooth and rough silver substrates were obtained by surface infrared and surface plasmon enhanced Raman spectroscopy. The assemblies were laid down by the Langmuir-Blodgett deposition technique. For Raman scattering the intensity of the incident light was enhanced by grating coupling to surface plasmon optical modes of the metal or to localized plasmon modes in the case of rough surfaces. It was found that the different vibrational frequency regions corresponding, for example, to C-C and C-H stretching modes, were enhanced by selecting different scattering angles for collecting the inelastically scattered light. The Raman spectra of monolayer assemblies in contact with silver islands showed evidence of conformational disorder, i.e., the alkyl chains of some molecules were not in the all-trans configuration. In contrast, the infrared spectra did not show evidence of similar disorder. These observations were explained by assuming that the infrared photons sensed the majority undistorted molecular species, while the Raman photons came from a distorted

*Permanent Address: Istituto di Chimica Fisica, Universita degli Studi di Padova, 2 Via Loredan, 35100 Padova, Italy

**Present Address, IBM Instruments Inc., 40 West Brokaw Road, San Jose, California 95110

***Permanent Address: Physik Department E22, Technische Universität München, D-8046 Garching, Fed. Rep. Germany

minority species located in regions where optical electromagnetic fields were enhanced by shape plasmon resonances of the rough silver surface.

I. INTRODUCTION

Surface plasmons (SPs) are collective oscillations of the conduction electrons in the surface region of a metal.[1] They are the counterparts of the well known volume plasmons of the 'free electron gas' of a metal. The importance of SPs in spectroscopy stems from the intense electromagnetic fields associated with these modes at optical frequencies. These fields can be used to characterize the optical properties of adsorbed layers of molecules. The combined system of electromagnetic field and oscillating surface charge is described best in terms of new modes called plasmon surface polaritons (PSPs), that are true collective electromagnetic modes of the interface between a metal and its surroundings. The characteristic frequencies of surface plasmons and the dispersion relation for the corresponding plasmon surface polaritons depend very strongly on the geometry of the interface.

For an infinite plane interface separating a free electron gas with dielectric function

$$\varepsilon_M(\omega) = 1-(\omega_P/\omega)^2 \tag{1}$$

from a non-dispersive material with dielectric constant ε_A, the surface plasmon has the frequency

$$\omega_{SP} = \frac{\omega_P}{\sqrt{1+\varepsilon_A}} . \tag{2}$$

The dispersion relation for PSPs in the same geometry is

$$\omega = ck_x(1/\varepsilon_M + 1/\varepsilon_A)^{1/2} , \tag{3}$$

where k_x is the surface propagation vector. In Eqs. (1) and (2) the quantity ω_P defines the frequency of the volume plasmon according to

$$\omega_P = (4\pi e^2\rho/m)^{1/2} , \tag{4}$$

where ρ is the free electron gas density. Analysis of the electromagnetic field equations describing PSPs shows them to be p-polarized (meaning their $\vec{E}$ field lies in the plane perpendicular to the surface and in the direction of propagation) and limited in frequency to the range $0 \leq \omega < \omega_{SP}$. The high field intensity associated with PSPs is seen in the expression for the magnetic vector

$$\vec{H} = H_0 \exp[i(k_x x - \omega t)] \exp(-\alpha |z|) \tag{5}$$

where in the dielectric ($z<0$) we set

$$\alpha \equiv \alpha_A = \left[k_x^2 - \varepsilon_A(\omega/c)^2\right]^{1/2}, \quad H_0 = -i(\omega\varepsilon_A/\alpha_A c)E_0 \tag{6}$$

and in the metal ($z>0$) we set

$$\alpha \equiv \alpha_M = \left[k_x^2 - \varepsilon_M(\omega/c)^2\right]^{1/2}, \quad H_0 = i(\omega\varepsilon_M/\alpha_M c)E_0 \,. \tag{7}$$

Notice that the exponential decay of $\vec{H}$ in both media ensures that the field has its maximum value at the surface; the position of any adsorbed layer. It is this property of all the field components of the PSP mode that makes it so useful in spectroscopic studies of adsorbed layers.

Because PSP modes of flat surfaces are non-radiative ($k_x > \omega/c$) they can be excited by light only by coupling techniques. The use of the evanescent fields of prisms to excite PSP modes is well known.[1] For Raman spectroscopy we have used the fact that the momentum mismatch between incident photon and PSP can be overcome through the use of surfaces weakly modulated in the shape of a grating.[2] This technique has some advantages, the primary one, in our experience, is the flexibility of being able to use direct front surface illumination without the need of an intervening prism as in either the Otto or Kretschmann configurations.[1,2]

The presence of a periodic grating on the metal surface imposes a Brillouin zone structure upon the dispersion curve of the flat surface PSP. Figure 1 shows schematically the dispersion of the flat surface PSP (heavy line and dots, segments I, II', III'', ...) and its modification due to a grating (thin solid lines) in the extended zone scheme, for positive values of surface wavevector k_x. The periodicity of the grating is Λ and the Brillouin zone boundaries are at $\pm n\pi/\Lambda$ ($n=1,2,3,...$). One may regard the dispersion curve within the first zone (segments II, III, IV, ...) as obtained by folding back the flat surface curve at the boundaries $\pm\pi/\Lambda$. In terms of the basic vector grating of the grating reciprocal lattice $k_g = 2\pi/\Lambda$, the boundaries of

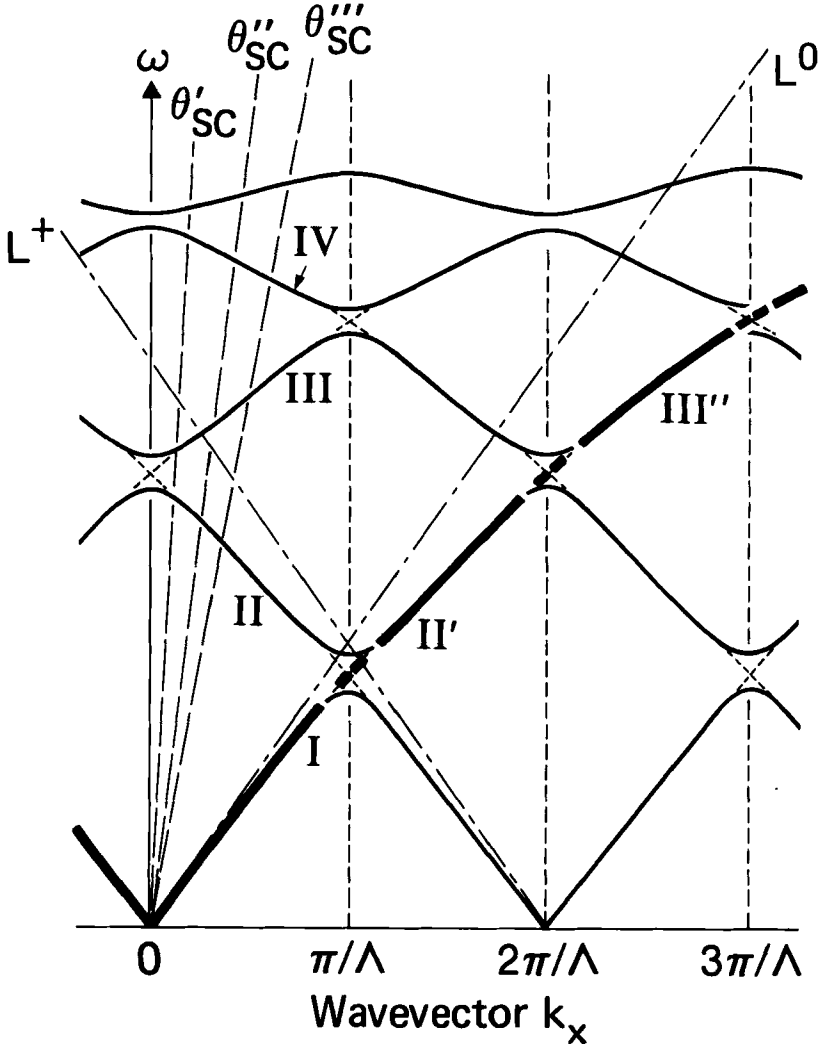

Figure 1. Schematic diagram showing the dispersion of a plasmon surface polariton (PSP) on a periodic grating. The gaps at $k_x = \pi/\Lambda$ ($n=0,1,2,...$) occur because of coupling between oppositely propagating surface polaritons. These couplings are mediated by multiples of the grating vector k_g. The principle light lines are L° and L^+. The branches of the PSP dispersion curve are labelled I, II, III, ..., etc. Scanning wavelength at constant angle corresponds to one member of the family of scan lines labelled θ'_{SC}, θ''_{SC}, θ'''_{SC}.

the first zone are at $k_x = \pm k_g/2$. The principal light lines are labelled L° and L^+ in Fig. 1. The PSP branches in the first zone are labelled I, II, III, ..., etc., the gaps at $k_x = \pm \pi/\Lambda$ separating branches I from II occur because of coupling between forward and backward propagating surface polaritons mediated by the grating vector k_g. Similarly, the gap at $k_x = 0$ separating branch II from III occurs because of coupling mediated by vector $2k_g$ between oppositely propagating surface polaritons. The dotted lines in the region of the gaps represent schematically the non-interrupted dispersion of the PSP on a flat surface.

The Raman measurements described in this paper are made by collecting the light emitted from the grating at a fixed angle, θ_{SC}. This is equivalent to traversing along one member of the family of dashed lines labelled θ'_{SC}, θ''_{SC}, or θ'''_{SC}, converging on the origin in Fig. 1. Each dashed line corresponds to a wavelength scan at a different θ_{SC}. Notice that each fixed angle scan cuts the PSP branches at a different set of energies so that making scans at many different angles allows one to map out the dispersion curve for the PSP on a grating.

In the experiments described here enhancements of the incoming and outgoing fields are physically separate since distinct PSP modes are involved. Thus grating experiments of this type, with controlled layer thicknesses, provide a means of separating the effect of PSP enhancement mechanisms for incoming and outgoing photons. This is of some interest in connection with surface enhanced Raman scattering from much rougher surfaces where it is believed that localized plasmon resonances also provide for enhancement of the ingoing and outgoing electromagnetic fields.[3]

II. GRATING PREPARATION

The gratings were produced holographically using a Krypton laser beam (Coherent CR 3000K) with wavelength $\lambda = 413.1$ nm. About 80 mW of laser power entered each of the two beam expanders in a dual beam interferometer arrangement. The recording material was a photoresist film (Shipley AZ-1350 B) spin-coated on optically polished fused silica substrates. To avoid the formation of "ghost gratings", reflections from the back side of the substrate were eliminated by applying a thick layer of a light absorbing lacquer. After an exposure time of 4 seconds the holograms were developed for 30 seconds in a solution of one part Shipley AZ-351 developer in three parts of water, then rinsed with water, and dried in a stream of

nitrogen. The photoresist layer now showed a surface profile corresponding to the sinusoidal intensity distribution which was present during the exposure. Finally, these holograms were covered with silver (thickness ca. 200 nm) at normal incidence in a standard laboratory evaporator.

To determine the grating constant Λ and the amplitude H of the metal gratings we measured the first order diffraction angle $\theta^{(1)}$ and grating efficiency $R_s^{(1)}$ for s-polarized light. The grating parameters were then calculated by comparing the measured values with the theoretical expressions given in Ref. 4. The efficiency for incident p-polarized light to excite PSPs depends strongly on the grating amplitude. Therefore, by varying the exposure time, we produced a series of gratings with different amplitudes and measured the resulting reflectivity minima $R_{p,min}^{(0)}$ with p-polarized light of wavelength λ=514.5 nm. Gratings where chosen that had a deep reflectivity minimum without too much broadening of the resonance. For the 'optimized' gratings used in our experiments we determined that $\Lambda \simeq 415$ nm and $H \simeq 10$ to 15 nm.

III. LANGMUIR FILM DEPOSITION

The layers were prepared by dissolving arachidic acid in distilled chloroform and spreading the solution on the surface of doubly distilled water. The water was buffered to a pH of 6.3 by the addition of $NaHCO_3$. After the evaporation of the chloroform, a closely packed monomolecular arrangement of the molecules with the hydrophilic end facing the water surface was formed when a surface pressure of typically 30 dyne/cm was applied. By lowering a silver coated glass slide slowly into the water, a monolayer could be transferred to a silver surface with the hydrophobic end of the arachidate pointing towards the silver. Alternatively by starting with the substrate in the lowered position before spreading and compressing the film, a monolayer could be transferred to a hydrophilic surface during withdrawal (see Fig. 2). The deposited layer consists of cadmium arachidate (CdAA) formed by a reaction of the fatty acid in the water and Cd^{++} ions from $CdCl_2$ dissolved in the water. By repeating the lowering and withdrawing procedure a layer of any given thickness can be formed.[5]

Substrates of evaporated Ag were prepared either as flat 100 nm thick films, sinusoidal gratings, or islands, approximately 10 nm thick, on quartz microscope slides. The technique of making gratings suitable for enhancement of Raman scattering was described

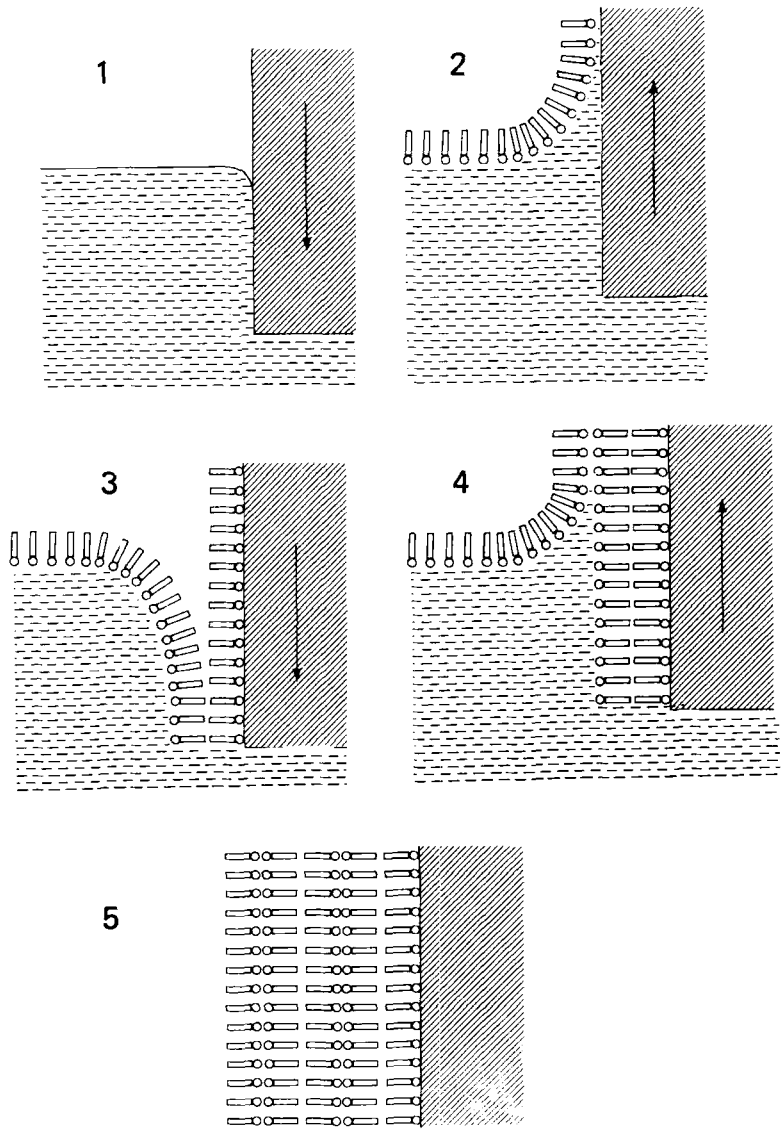

Figure 2. Schematic diagram illustrating the procedure for depositing monolayers on a hydrophilic surface. First the substrate slide is lowered into the *Langmuir-Blodgett* trough. On spreading from a solution the monolayer onto the water surface and compressing it with a float, the substrate is slowly drawn out of the water and a monolayer transferred. Subsequent dippings transfer two layers first to the hydrophobically created surface on the down motion and then to the hydrophilically created surface on the up motion.

briefly in the last section. The CdAA layers were deposited on these substrates by the Langmuir-Blodgett monolayer deposition technique such that the initial layer was deposited in either the "head down" (carboxylate closest to the Ag surface) or "tail down" (terminal methyl closest to the Ag surface) configuration. The thickness of the deposited organic film was checked by measuring the shift in the plasmon surface polariton (PSP) reflection minimum. In some experiments, after the Raman or infrared spectra of these assemblies were obtained, the CdAA was sandwiched by additional evaporation of Ag, as islands or continuous films, on top of the CdAA monolayer assembly.

IV. RAMAN SPECTRA FROM MONOLAYER ASSEMBLIES ON GRATINGS AND ROUGH METAL SURFACES

The Raman scattering was excited with green light 530.9 nm of a Krypton ion laser (Coherent radiation model CR 3000K) and dispersed through a Spex 14018 double monochromator. The detector was a thermoelectrically cooled PMT (RCA 31034 A); the photon counting electronics a commercial Spex DPC-2 system. The spectrometer was computer controlled with a repetitive scanning for coaddition of spectra.

Figure 3 shows a set of spectra taken under identical conditions except for the angle at which the inelastically scattered light was collected. The sample consisted of a silver grating overcoated with twentyeight monolayers of CdAA. The p-polarized exciting laser (λ_L=530.9 nm, power 120 mW) was incident at θ_i=17° corresponding to the reflectivity minimum due to grating PSP modes of this coated grating. Slit widths 600 μm, full scale 5000 cps, step size 10 cm^{-1}. The spectra consist of two very broad peaks, indicated by the shading, and a collection of sharp bands corresponding to the Raman vibrational modes of the adsorbed CdAA assembly. Resolution of the latter was limited by the step-size (10 cm^{-1}) chosen to record these spectra in a reasonable time period.

It is now well established experimentally that metal gratings on silver and gold can emit light and that this light arises from radiative PSP modes.[6-8] That the two broad emission bands in Fig. 3 are due to PSP luminescence is implied by the earlier observations, and the fact that when their absolute energy is plotted against angle of observation, one obtains the dispersion of a grating PSP near the zone center. In earlier experiments with Au gratings[7] we could not map out the $k_x \simeq 0$ region because the PSP was damped out by the

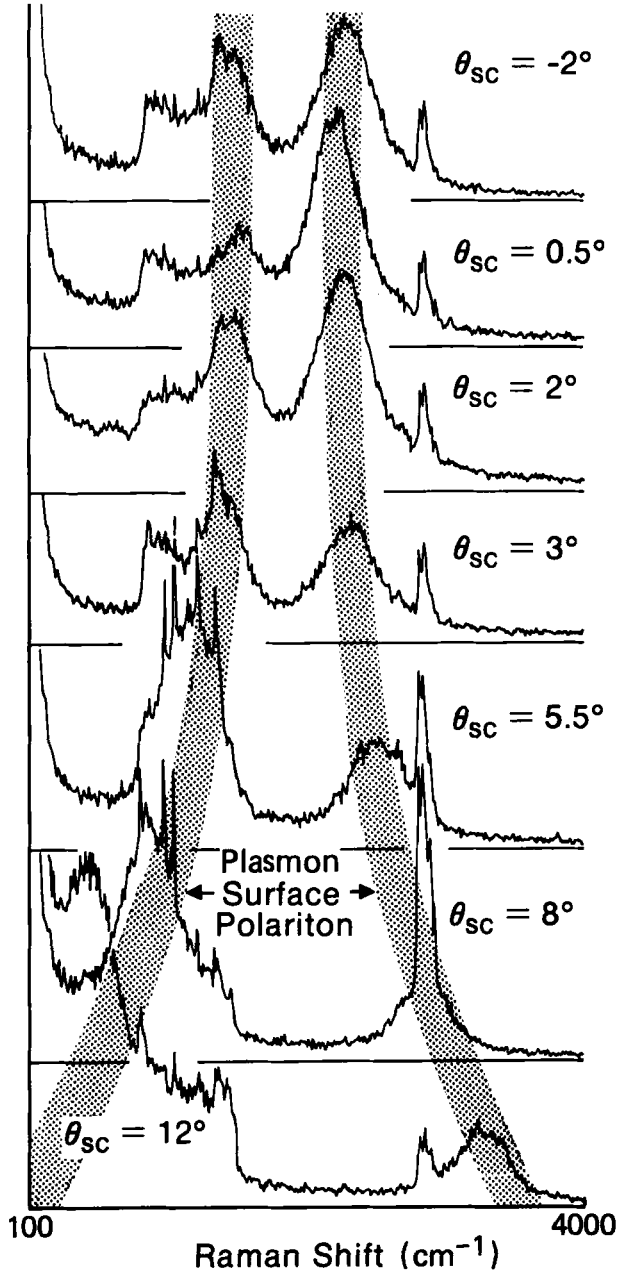

Figure 3. Luminescence and Raman scattering from a silver grating coated with 28 monolayers of CdAA for different scattering angles θ_{SC}.

interband transition. The expected downward shift in the dispersion was also evident in the data. Examining Fig. 3 starting with the top panel, we note that the PSP luminescence peaks first move together and then apart (θ_{SC}=-2,0.5,2°) just as expected for PSP modes on branches II and III near the zone center gap (see Fig. 1).

The second noticeable feature in the spectra displayed in Fig. 3 is associated with the CdAA Raman bands. These clearly become much more intense whenever the direction of the Raman scattered light also corresponds to the direction of the PSP luminescence. The effect is seen most clearly in the C-H stretching region near 2900 cm^{-1}. It appears that as the luminescence peak due to the PSP on branch II sweeps by the C-H stretching bands the latter become enhanced by a factor that is not quite an order of magnitude. This effect is due to the PSP enhancement of the out-coupled Raman field.

Raman spectra have also been measured for monolayer assemblies deposited on a variety of rough metal surfaces, such as island films, and sandwiched between flat or grating surfaces and an island film. In Fig. 4, we display a selection of representative spectra for the C-H stretching modes, together with a schematic, showing the type of sample used. Note that unlike the infrared spectra depicted in Fig. 5, there is no sample corresponding to arachidate layers on a flat smooth metal surface. This is because Raman scattering is a weak process and one needs an enhancement mechanism in order to see one monolayer on a highly reflecting metal like silver.

Figure 4A shows the Raman spectrum of eleven monolayers of arachidate on a metal grating. Direct excitation of the plasmon surface polariton insures that the signal is enhanced sufficiently that it becomes possible to record the Raman spectrum. The grating constant Λ (ca. 415 nm) is large enough relative to the modulation height H (ca. 10 nm) for us to reasonably presume that the monolayers follow the sinusoidal oscillation of the surface without too much disturbance of both packing and chain configuration. It has been observed within experimental error that the intensity of the $d^-(0)$ mode at ca. 2880 cm^{-1} increased linearly with number of monolayers in the region n=2 to 12. This supports the conclusion that the spectrum shown is representative and is free of any additional enhancement beyond that due to PSP's on the grating. The peak height ratio $I_{2850}/I_{2880} \simeq 1.4$ measured from the continuous background evident outside the interval (2830 cm^{-1}, 2990 cm^{-1}) is typical for structures like phospholipid bilayers below their order-disorder transition temperature.[9] These molecules also have similar lengths when their alkyl chains are extended in the all trans form. We conclude that Fig. 4A is representative of a

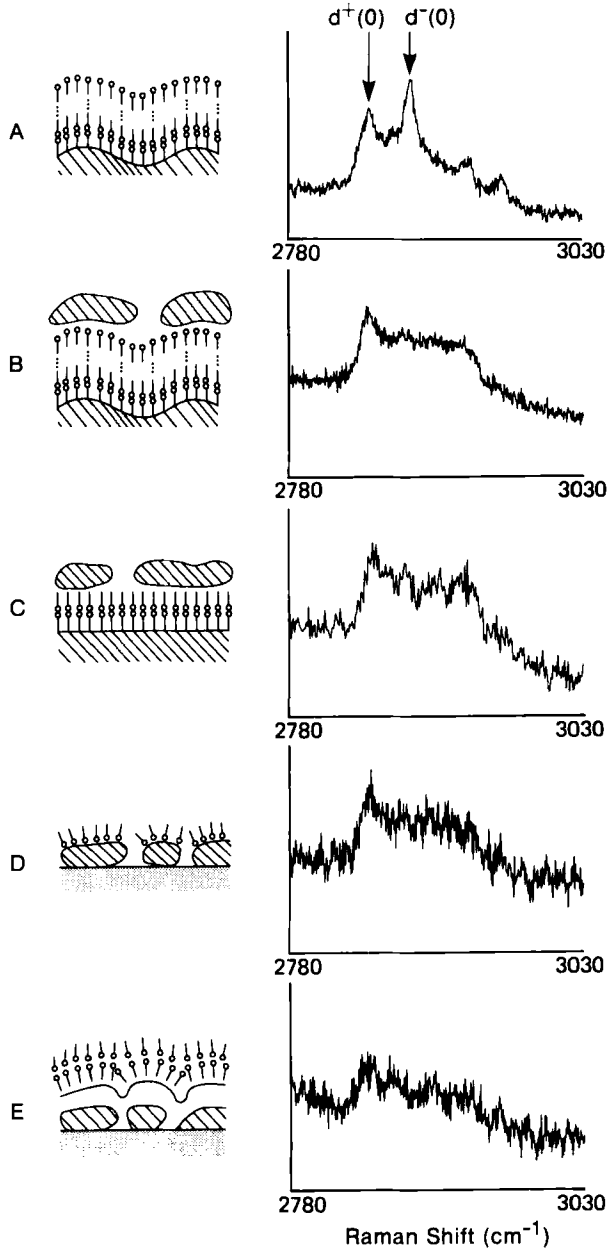

Figure 4. Raman spectra of monolayer assemblies on a variety of rough Ag surfaces. See the text for a detailed description.

conformationally ordered monolayer assembly on a flat surface. The attenuated total reflection (ATR) scans consisting of the p-polarized reflectivity as a function of angle taken at constant wavelength $\lambda_L = 632.8$ nm showed that the reflection minimum due to the PSP on the coated grating was well defined and sharp. The shift between films of different thickness was just that expected for monolayer assemblies on flat metal surfaces and the angular position of the minimum is close to that expected by folding the dispersion curve of the flat surface at the Brillouin zone boundary. Furthermore, the width and depth of the assemblies resemble the flat metal case sufficiently to rule out the occurrence of any differences in thickness that would imply gross disorder for the films on the grating.

The effect of evaporating a 10 nm island film of Ag on top of eleven arachidate layers is shown in Fig. 4B. Note that the $d^-(0)$ mode at ca. 2880 cm^{-1}, which is prominent in powder spectra is practically absent. There is a strong spectral resemblance between Fig. 4B and spectra for liquid phase fatty acid samples. Scanning electron micrographs showed the presence of the grating clearly visible beneath the film of irregularly shaped islands with average size of the order 50 nm. However, the p-polarized PSP resonance minimum visible before depositing the metal islands was barely detectable because it was so broad. The Raman signal from the island sample was approximately four times larger than before thereby burying the original spectrum. This enhancement is interpreted as surface Raman from the high electromagnetic field regions in the immediate vicinity of the islands.

Figure 4C shows the Raman spectrum of two arachidate layers sandwiched between a flat evaporated metal film and island film of Ag. The Raman signal is very similar to that in Fig. 4B, implying that the signal is from an ensemble with similar conformation and packing. Likewise, when monolayers were deposited directly on top of an island film, the Raman spectrum, Fig. 4D, was again characteristic of conformationally disordered samples. Since the metal surface has approximately the same topography as the islands, the Raman scattering is assumed to originate from conformationally disordered regions of the layers.

In samples with deposited silver islands, the intensity of the signal was found to be approximately independent of the number of layers deposited, i.e., there was no indication that the Raman signal increased as the number of layers was increased. This supports the idea that the signal comes from a very localized set of molecules, which may in fact, be a collection closest to the island surface and that this effect is therefore indicative of a SERS effect. The SEM

pictures of the samples used for Fig. 4D showed that these islands were well formed and not as irregular as those created on top of CdAA arachidate layers in Figs. 4B and 4C. Even so there were no clear differences between spectra in 4C and 4D. Island films in Fig. 4D were discontinuous so that CdAA could have been exposed to metal and glass surfaces. That this had little effect on the Raman signal from the C-H stretching region was shown by Fig. 4E which displays the spectrum from two layers of CdAA deposited on top of a continuous metal film that had been evaporated in such a way as to cover a pre-existing island film (see schematic on the left-hand side).

V. INFRARED REFLECTION ABSORPTION SPECTRA OF MONOLAYER ASSEMBLIES

Single reflection, grazing incidence infrared spectra of the monolayer samples on flat Ag substrates, with and without Ag island overlayers, in the C-H stretching mode region were obtained by infrared reflection-absorption spectroscopy.[10] In these measurements infrared radiation from a standard Nernst glower was first modulated by a rotating blade chopper at ca. 200 Hz and focused onto the sample at grazing incidence (ca. 85°). The reflected radiation was then passed through a CaF_2 photoelastic modulator/fixed wire grid polarizer assembly (114 KHz) and then focused onto the slits of a 1/2m grating monochromator. The output of the monochromator was then focused onto a liquid nitrogen cooled InSb photovolatic detector. IR spectra of CdAA assemblies on flat Ag surfaces were also reported in Ref. 11.

If we define I_p and I_s as the intensity of the radiation polarized parallel and perpendicular to the plane of reflection of the sample, respectively, then this double modulation scheme allows, upon phase sensitive demodulation of the detector output, simultaneous recording of (I_p+I_s) and (I_p-I_s). The final output of the spectrometer was recorded as the ratio of these two quantities, $(I_p-I_s)/(I_p+I_s)$, as a function of wavelength. Since I_p and I_s were, on the average, absorbed to the same extent throughout the spectrometer optics, but only I_p was effectively absorbed by the surface species, the spectra of gas phase molecules, spectrometer optics, etc., canceled when the ratio was taken and only the spectrum of the oriented layer was recorded. Complete details of this technique can be found elsewhere.[12]

Figure 5 summarizes the infrared spectra of monolayers and multilayers of CdAA on smooth and rough metal surfaces for the C-H stretching mode region between 2800-3000 cm^{-1}. On the left-hand

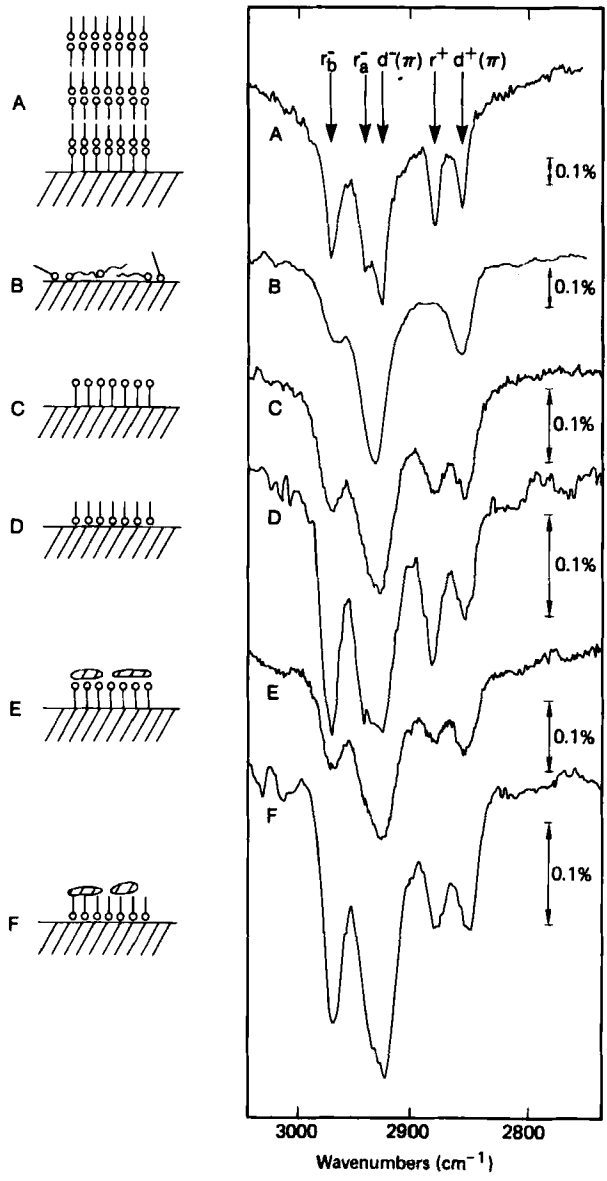

Figure 5. Infrared spectra of monolayer assemblies on a variety of rough surfaces. See the text for a detailed description.

side is depicted schematically the system whose infrared spectrum is shown on the right-hand side. Figure 5A shows the infrared absorption of six layers of CdAA on a flat Ag surface obtained by conventional FTIR spectroscopy[13] using an IBM Instruments IR/98 spectrometer. In Fig. 5A, five bands are visible at: 2850 ($d^+(\pi)$,$\nu_s(CH_2)$), 2874 (r^+,$\nu_s(CH_3)$), 2918 ($d^-(\pi)$,$\nu_a(CH_2)$), 2933 (r_a^-,$\nu_a(CH_3)$) and 2962 (r_b^-,$\nu_a(CH_3)$) cm^{-1}. Note that $d^-(\pi)$ and r_a^- are not easily distinguished in spectra B through F.

We note that in Fig. 5A, unlike the infrared spectrum of CdAA powder the apparent intensities of both $d^+(\pi)$ and $d^-(\pi)$ are attenuated substantially relative to r^+ and r^-. This is due to the well known surface selection rule for the infrared.[14] Since the structure of this six-layered CdAA film is such that $d^+(\pi)$ and $d^-(\pi)$ are directed almost entirely perpendicular to the E vector of the incident light, the absorbance of these modes is attenuated. Spectrum 5A is thus representative of a well ordered surface layer of CdAA. Figure 5B shows the infrared spectrum of an alumina substrate dipped into a 10^{-3} molar solution of arachidate acid, rinsed thoroughly with solvent and air dried.[15] Radiolabel studies have shown that coverages approximately one monolayer or less are obtained in this fashion. This layer is neither closest packed as expected for a compressed monolayer nor are all the chains likely to be in an all trans configuration. Consequently, this spectrum may be regarded as representing a system with intra and intermolecular disorder. Further, since there is no reason to expect the hydrocarbon backbones of the molecules to be aligned along the surface normal, this spectrum is representing a disordered CdAA surface layer.

Figures 5C and 5D show the infrared spectrum of one monolayer of CdAA deposited on a flat silver substrate in the tail-down and head-down configurations, respectively. The band peaks are at essentially the same positions for both samples. The relative intensities of $d^+(\pi)$ to r^+ and $d^-(\pi)$ to r_b^- in Figs. 5C and 5D are slightly different and to the corresponding ratios in spectrum 5A. If the gross structure of these layers can be truely represented by the ball-and-stick schematics shown in Fig. 5, then differences in these ratios for the various films are significant. They could represent structural differences due to an overall off-normal tilt of the hydrocarbon backbones, or possibly some few percent of the total film in the gauche form.

Figures 5E and 5F show the infrared spectrum after evaporating a 10 nm Ag film on top of the tail-down and head-down samples, respectively, under conditions that yield an island Ag film. Note that there is essentially no change in the spectra of the head-down or

tail-down samples as a result of this treatment. The Raman spectrum of the same tail-down sample was found to be essentially the same as that in Fig. 4C. It, by contrast, is indicative of conformational disorder. Clearly, the two spectroscopic techniques are monitoring different ensembles within the same sample.

The main point to emphasize is that the Raman and infrared spectra of directly comparable samples indicate that different ensembles are being observed. The presence of silver surface roughness in the form of islands changes the Raman spectrum. No such effect is apparent in the infrared spectra. Thus, spectra 5E and 5F for a monolayer under an island film are not very different from 5C and 5D, respectively. However, their counterparts in Raman, namely spectra 4A and 4B are very different. From signal to noise considerations in the infrared spectra we estimate that less than ten percent of the monolayers are perturbed by evaporating a 10 nm Ag film on top. Consequently, we conclude that the Raman signal for samples with island-like topographies is due to a SER effect from a minority species, whereas the infrared is from a majority species in ordered regions of the monolayer assembly.

ACKNOWLEDGMENTS

We thank M. Jurich, R. Santo and J. Escobar for technical assistance, and J. Rabolt for discussions concerning assignments.

REFERENCES

1. For a review of plasmon surface polaritons, see H. Raether, Surface Plasma Oscillations and Their Applications (Academic, New York-London, 1977); *Physics of Thin Films* **9**, 145-261 (1976), and references therein.
2. A. Girlando, M. R. Philpott, D. Heitmann, J. D. Swalen and R. Santo, *J. Chem. Phys.* **72**, 5187 (1980).
3. For a review see, "Surface Enhanced Raman Scattering," edited by R. K. Chang and T. E. Furtak (Plenum Press, NY, 1982).
4. D. Heitmann, *Opt. Commun.* **20**, 292 (1977).
5. H. Kuhn, D. Möbius and H. Bücher, in Physics Methods of Chemistry, edited by A. Weissberger and B. W. Rossiter, (Wiley Interscience, New York, 1972), Part IIIB, Chap. VII.
6. J. C. Tsang, J. R. Kirtley and T. N. Theis, *Solid State Commun.* **35**, 667 (1980).

7. A. Girlando, W. Knoll and M. R. Philpott, *Solid State Commun.* **38**, 895 (1981).
8. W. Knoll, M. R. Philpott, J. D. Swalen and A. Girlando, *J. Chem. Phys.* **75**, 4795 (1981).
9. R. G. Snyder, S. L. Hsu and S. Krimm, *Spectrochimica Acta* **34A**, 395-406 (1978).
10. W. Knoll, M. R. Philpott and W. G. Golden, *J. Chem. Phys.* **77**, 219 (1982).
11. D. Allara and J. D. Swalen, *J. Phys. Chem.* **86**, 2700 (1982).
12. W. G. Golden, D. S. Dunn and J. Overend, *J. Catal.* **71**, 395-404 (1981).
13. J. F. Rabolt, F. C. Burns, N. Schlotter and J. D. Swalen, "Anisotropic Orientation in Molecular Monolayers by Infrared Spectroscopy," *J. Chem. Phys.*, in press (1982).
14. H. A. Pearce and N. Sheppard, *Surf. Sci.* **59**, 205-217 (1976).
15. W. G. Golden, C. Snyder and B. Smith, *J. Phys. Chem.*, in press (1982).